Pseudo-cubic crystal structure and phase transition in doped ye'elimite

Ana Cuesta[†], Ángeles G. De la Torre[†], Enrique R. Losilla[†], Isabel Santacruz[†], Miguel A. G. Aranda*[†] [#]

[†] Departamento de Química Inorgánica, Cristalografía y Mineralogía, Universidad de Málaga, 29071-Málaga, Spain.

[#] ALBA Synchrotron, Carretera BP 1413, Km. 3.3, E-08290 Cerdanyola, Barcelona, Spain

KEYWORDS: Sodalite structure, Rietveld method, synchrotron powder diffraction, phase transition

Supporting Information Placeholder

ABSTRACT: Sodalites are tridimensional alumino-silicate materials containing cages where loosely bonded anions are located. Ye'elimite, $Ca_4[Al_6O_{12}]SO_4$, is outstanding as an aluminate sodalite with a flexible framework accepting several type of dopants with important structural consequences. Moreover, ye'elimite is also important from an applied perspective as it is the most relevant phase in calcium sulfoaluminate cements. The crystal structure of stoichiometric ye'elimite has recently been unraveled but the structure of dopant-containing ye'elimite, which is presents in cements, is not well studied. Here, we report the pseudo-cubic crystal structure of doped ye'elimite, $Ca_{3.8}Na_{0.2}Al_{5.6}Fe_{0.2}Si_{0.2}O_{12}SO_4$, from high-resolution synchrotron powder diffraction data. The powder pattern is indexed with a cubic cell and a structural model is reported based on the $I\bar{4}3m$ space group. However, this compound displays diffraction peak narrowing on heating. Furthermore, some high-angle split peaks become single peak on heating and a phase transition is measured at 525ºC. Therefore, it is concluded that the crystal structure at room temperature has lower symmetry although it can be described as cubic. The structural study at 800ºC suggests a truly cubic structure and we speculate that this phase transition, on heating, is likely related with the dynamical disordering of the sulfate anions. Finally it is concluded that the high temperature cubic state was not quenchable to ambient, even when the tested chemical substituents are introduced into the structure.

INTRODUCTION

Sodalites with general composition $M_4[T_6O_{12}]X$ have been known for many years as both naturally-occurring minerals and synthetic compounds[1]. The general formula refers to a structure that is (ideally) a body-centered cubic unit cell with a lattice parameter of 9 Å and where M is a relatively low-charged caged cation such as Ca, Na or Sr[2]; T occupies tetrahedral site(s) and is typically Si or Al; and X is the loosely-bonded caged anion which is either spherical (in the case of Cl) or tetrahedral (in the case of SO_4, WO_4, and CrO_4). Sodalites are interesting materials for several reasons such as their ferroic phase transition[3] from the high-temperature cubic phase to complex superstructures at lower temperatures.

Stoichiometric calcium sulfoaluminate or ye'elimite, $Ca_4[Al_6O_{12}]SO_4$, can be described as a sodalite where M = Ca, T = Al, and X =SO_4, and crystallizes as a tectoaluminosilicate sodalite structure[4]. This structure was first analyzed by Hanstead and Moore[5] using X-ray powder diffraction,[6] and Saalfeld and Depmeier[7] reported atomic parameters for a cubic crystal structure with space group $I\bar{4}3m$ and a=9.195 Å. In 1995, Calos et al.[8] published an orthorhombic crystal structure, Pcc2 space group, which was revised in 2013 by joint neutron and X-ray powder diffraction Rietveld refinement and atomistic calculations[4]. Recently, the disordered crystal structure of cubic stoichiometric ye'elimite at 800ºC has been satisfactorily studied in the $I\bar{4}3m$ space group using a split-atom model[9].

Stoichiometric ye'elimite at room temperature is orthorhombic Pcc2. However, the substitutions of Ca^{2+} by Na^{+} and Al^{+3} by B^{3+}, Si^{4+} or Fe^{3+} seems to restore the cubic symmetry[10]. In the case of iron, its maximum substitution degree may depend on the crystal structure of ye'elimite[5], due to the competition between aluminum and iron. Idrissi et al.[11] studied the Al/Fe substitution, $Ca_4Al_{6-2x}Fe_{2x}SO_{16}$, where x was comprised between 0 and 3, and other authors found that the maximum iron solid solution was reached at 22.61 wt%, expressed as Fe_2O_3[12]. The polymorphism of ye'elimite and its solid solutions in the presence of different amounts of Na^{+} and Fe^{3+} were also investigated[13].

In addition, the interest in the ye'elimite structure has recently increased because it is the major component in calcium sulfoaluminate cements (CSA)[14-16], and the second most relevant phases in sulfobelite cements, BCSA, (~25 wt%)[17-19]. CSA and BCSA cements are environmentally-friendly materials as they allow decreasing the CO_2 footprint in cement fabrication. On average, for every ton of ordinary Portland cement (OPC) produced, 0.97 tons of CO_2 are released into the atmosphere[20,21], with the cement industry contributing around 6% of all anthropogenic CO_2 emissions. By comparison, CSA cements are produced with significantly lower CO_2 emissions relative to OPC, achieved through the use of lower amount of carbonated raw-materials (part of calcite is replaced by gypsum) and a reduced clinkering temperature. The overall CO_2 emission reduction can amount up to 40%.[21]

The effect of iron in the formation of ye'elimite in belite calcium sulfoaluminate clinkers has been also studied[22,23]. The iron content of ye'elimite in these industrially produced clinkers was analyzed and it resulted relatively low[24,25]. In a recent work[22], orthorhombic and cubic ye'elimite polymorphs were observed to occur in BCSA clinkers doped with B^{3+} and Na^{+}.

However, the ye'elimite phase was cubic when Na^+, Fe^{3+} and Si^{4+} were simultaneously present. Bullerjahn et al.[23] also found a mixture of cubic and orthorhombic ye'elimite in their cements and the cubic polymorph increased at the expense of the orthorhombic one with increasing the iron content. A reverse correlation between the amount of ye'elimite and tetracalcium aluminoferrite (C_4AF) was found, which agrees with the incorporation of iron into ye'elimite framework[23].

The structure of stoichiometric ye'elimite has been recently established as orthorhombic[4] at room temperature and cubic[9] at high temperatures. The objective of this study is to clarify the crystal structure of doped (disordered) ye'elimite. To this end, highly crystalline single phase iron-silicon-sodium doped ye'elimite, $Ca_{3.8}Na_{0.2}Al_{5.6}Fe_{0.2}Si_{0.2}O_{12}SO_4$, has been synthesised. The high temperature structure and phase transition have been studied by thermodiffractometry. At 800ºC, doped ye'elimite seems to be truly cubic. At room temperature, synchrotron powder diffraction also indicates a cubic diffraction pattern. However, the thermodiffractometric study shows peak narrowing with some high-angle partially split peaks (at room temperature, RT) becoming single peaks (after a phase transition measured at 525 ºC). Therefore, we are forced to conclude that the RT structure is pseudo-cubic. The reported RT structure is important from both basic (f.i. phase transitions) and applied research (cement analysis) points of views.

EXPERIMENTAL SECTION

Synthesis conditions.

Doped ye'elimite with a nominal composition of $Ca_{3.8}Na_{0.2}Al_{5.6}Fe_{0.2}Si_{0.2}O_{12}SO_4$ was synthesized following the methodology reported elsewhere[4] for stoichiometric ye'elimite. Suitable amounts of $CaCO_3$ (99.95%, Alfa Aesar), Al_2O_3 (99.997%, Alfa Aesar), Fe_2O_3 (99.945%, Alfa Aesar), SiO_2 (99.56%, ABCR), Na_2CO_3 (99.999%, Sigma Aldrich) and $CaSO_4{\cdot}2H_2O$ (ground natural single-crystal from Málaga, Spain) were used to obtain approximately 8 g of powder. The mixture was ground for 1 hour in an agate mortar with ethanol. The resulting powder was dye-pressed (20 mm diameter and 500 MPa) and heated at 1250ºC for 4 hours (heating rate of 5 ºC/min) followed by a rapid cooling. Finally, the sample was ground in a tungsten carbide mortar.

Synchrotron X-ray powder diffraction (SXRPD).

SXRPD data was collected in Debye-Scherrer (transmission) mode using the X-ray powder diffraction station of ALBA, the Spanish Synchrotron Radiation Facility (Barcelona, Spain)[26]. The wavelength, 0.6202(2) Å, was selected with a double-crystal Si (111) monochromator and determined from a Si640d NIST standard (a=5.43123 Å) measurement. The diffractometer is equipped with a detector system based on crystal analyzers in the diffracted beam especially suited for high-resolution experiments giving also a flat background. The capillary (0.5 mm of diameter) was rotated at 400 rpm during data collection to improve diffracting particle statistics. The data acquisition time was very large, ~4 hours, to attain a very good signal-to-noise ratio over the angular range 1-45º (2θ). The temperature inside the experimental hutch was 26(1)ºC.

Analysis of SXRPD data.

Rietveld analysis was performed using the GSAS suite of programs and the EXPGUI graphic interface[27]. Final global optimized parameters were: background coefficients, zero-shift error, cell parameters, and peak shape parameters using a pseudo-Voigt function corrected for axial divergence[28]. We used as starting model the recently reported high temperature cubic structure[9]. The atomic positional coordinates and anisotropic atomic displacement parameters (ADPs) of ye'elimite were optimized.

Variable Temperature Laboratory X-ray Powder Diffraction (VT-LXRPD).

VT-LXRPD data were recorded on an X'Pert PRO MPD diffractometer (PANalytical) equipped with a Ge (111) primary monochromator, using strictly monochromatic $CuK\alpha_1$ radiation (λ=1.54059 Å) and an X'Celerator detector for the sample mixed with NIST silicon in order to decorrelate the thermal expansion from the sample height changes as a function of temperature. The sample stage was an Anton Paar HTK1200 camera working under static air. Data were collected with temperature interval ranging of 100ºC, from RT to 800ºC after a delay time of 15 min to ensure thermal equilibration. Data were acquired over the angular range 10-78º (2θ) with a step size of 0.017º, resulting in 2 hours acquisition time per pattern. The sample was then cooled to RT where a final RT pattern was also recorded. A Rietveld study was carried out as described above to extract the unit cell variation, the sample height changes and the peak shape evolution with temperature.

A higher quality pattern was collected at 800ºC in the range 5-100 (2θ) with a step size of 0.017º, resulting in a 6 h data collection time but for the pure sample (i.e. without added silicon). A Rietveld structural study was also perform on this pattern following the methodology detailed in the previous section.

Permittivity measurements.

Electrical characterization was carried out on cylindrical pellets (~10 mm in diameter and ~1 mm thickness) obtained by dye-pressing ~0.1 g of powders mixture at 500 MPa. The pellets were sintered at 1250ºC for 2 h after a heating rate of 5 ºC/min. Electrodes were made by coating opposite pellet faces with METALOR® 6082 platinum paste and heating to 800ºC at a rate of 5 ºC/min for 15 min in air to decompose the paste and to harden the Pt residue. Impedance data were collected using a Hewlett-Packard 4284 A impedance analyzer over the frequency range 20 Hz – 1 MHz from 300 to 700ºC at a heating rate of 10 ºC/min.

Results and Discussion

Synthesis.

Several stoichiometries were tested and the selected one is that with the highest dopant contents but yielding a single phase sample. The synthesis procedure followed to prepare doped ye'elimite, $Ca_{3.8}Na_{0.2}Al_{5.6}Fe_{0.2}Si_{0.2}O_{12}SO_4$, was very similar to that reported for stoichiometric ye'elimite[4], but the temperature

was reduced 50ºC relative to the synthesis temperature for stoichiometric ye'elimite, due to the presence of iron oxide in the reaction medium. The addition of SiO_2, Na_2O and Fe_2O_3 stabilized the high temperature cubic form of ye'elimite at room temperature.

Structural study of doped ye'elimite at room temperature.

SXRPD was used to study the crystal structure of doped ye'elimite, $Ca_{3.8}Na_{0.2}Al_{5.6}Fe_{0.2}Si_{0.2}O_{12}SO_4$. The high-resolution SXRPD pattern was auto-indexed using DICVOL06[29] in a cubic unit cell by using 20 lines. This cell indexes all observed diffraction reflections. Table 1 shows the auto-indexing results, including the figures of merits[30].

Table 1. Values for the unit cell for doped and stoichiometric ye'elimite cubic samples auto-indexed with DICVOL06, including figures of merit[30].

	a(Å)	V (Å^3)	T(ºC)	M(20)	F(20)
Doped-ye'elimte SXRPD	9.1974(7)	778.0	26	58.4	116
Doped-ye'elimte LXRPD	9.2533(1)	792.3	800	281	200
Stoich.-ye'elimte LXRPD	9.2475(1)	790.8	800	449	343

We have used the cubic crystal structure recently reported for stoichiometric ye'elimite at 800ºC[9], space group $I\bar{4}3m$, as starting model for the Rietveld refinement. Once the overall parameters were optimized, the structural parameters were varied. No attempts to locate the dopants have been carried out as they should be disordered in the cubic structure. The final Rietveld disagreement factors are shown in Table 2 where they are compared to those obtained for previous RT cubic[7] and HT cubic structures[9]. The recorded pattern clearly contains the diffraction reflections of the cubic sodalite structure. Furthermore, when tetragonal and orthorhombic symmetries were tested, the disagreement values were very high and the refinements did not converge. Figure 1 shows the SXRPD Rietveld plot using the refined cubic structure.

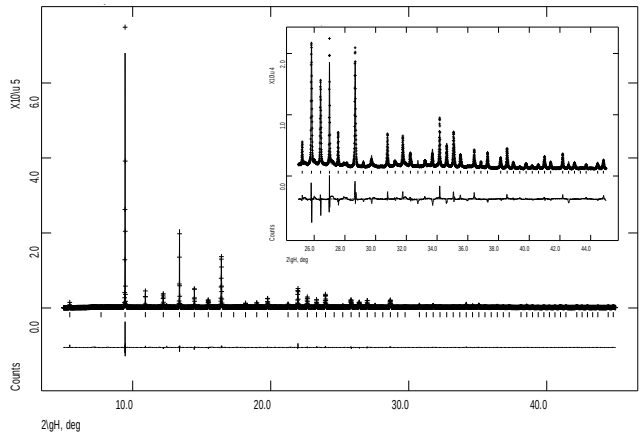

Figure 1. SXRPD Rietveld plot for the cubic structure of doped ye'elimite at RT. Inset details the high-angle range.

The refined unit cell parameter is a=9.1970(1) Å and the cell volume is 777.93(2) Å^3. The anisotropic displacement parameters (ADPs) were also optimized as in reference 9. The refined atomic parameters (coordinates and anisotropic displacement parameters) for the RT cubic structure of doped ye'elimite are given in Table S1, provided as supplementary information. Selected interatomic distances and angles are given in Table S2 (supplementary information). The AlO_4 tetrahedrons have four 1.734(1) Å bond distances and somewhat distorted angles with four values of 105.6(1)º and two large one, 117.4(2)º. The SO_4 tetrahedron is described by the oxygen split model[9] which lead to reasonably S-O bond distances of 1.474(6) Å. Unsplit oxygen-sulfate models invariably lead to much shorter, unrealistic, S-O bond distances. The corresponding CIF file is also deposited.

Table 2. Agreement factors for the Rietveld refinements of SXRPD and HT-LXRPD patterns for doped and stoichiometric ye'elimite cubic samples by using previously-reported cubic structures, references 7 and 9, and after atomic parameter refinement.

		Structure-1[7]		Structure-2[9]		This study	
	T /ºC	R_{WP} /%	R_F /%	R_{WP} /%	R_F /%	R_{WP} /%	R_F /%
Doped- SXRPD	26	19.9	17.4	15.4	16.9	11.0	7.9
Doped-LXRPD	800	14.4	16.7	6.6	4.4	5.8	3.0
Stoichiometric-LXRPD	800	22.6	19.5	11.4	6.5	9.9	3.2

Variable-temperature study and phase transition.

A VT-LXRPD study, up to 800ºC, was performed for doped ye'elimite. The full termodiffractometric study is reported in supplementary information, Figure S1, and Figure 2 shows two selected high-angle regions. Fig. 2.a displays the sharpening of the (622) reflection which was slightly split at room temperature and becomes a single sharp peak at high temperatures. Fig. 2.b shows the sharpening of the peaks at 75.8 º (2θ) which corresponds to the (721), (552) and (633) reflections which are intrinsically overlapped for cubic symmetry. Fig. 2.b also shows the thermal evolution of the (331) reflection of silicon for the sake of comparison which does not show any appreciable width change with temperature. All attempts to index the low temperature patterns with symmetry lower than cubic were fruitless as the observed splitting at high angles was very small and only observable for some diffraction reflections.

On the other hand, changes in the widths of the diffraction peaks with temperature were clearly measurable. Figure 3 plots the FWHMs (Full Width at the Half Maximum) values for the thermodiffractometric study including the data for ye'elimite and silicon. Figure 3 shows that the FWHM variation with temperature for Si is negligible. However, a very clear sharpening for doped ye'elimite up to 500 ºC is measured and then, the FWHM changes are negligible.

Figure 4 shows the refined volume as a function of temperature of the doped phase obtained from VT-LXRPD patterns combined with Rietveld analysis. Selected Rietveld plots on heating are deposited in supplementary information: Figures S2 to S6. The volumetric thermal expansion parameter (α_v) was calculated by fitting the data with a linear equation V=n+mT, where α_v=m/n. The linear coefficient of thermal expansion for a cubic system is defined as $\alpha_L=\alpha_v/3$. The final α_L values of this sample, assuming cubic structure, were $6.6\cdot10^{-6}$ ºC^{-1} (20-400ºC interval) and $9.0\cdot10^{-6}$ ºC^{-1} (500-800ºC interval), which are similar to values found for aluminosilicate sodalites[31]. In the case of the stoichiometric sample, a linear thermal expansion coefficient was calculated for each unit cell

parameter[32] (in the temperature range of 20 to 450ºC), Table 3. The coefficient was also calculated for stoichiometric ye'elimite (between 500 and 800ºC), Table 3, for the cubic structure. From this study it is concluded that doped ye'elimite has similar thermal expansion values to stoichiometric ye'elimite. From the VT-LXRPD study, the thermal expansion coefficient calculated for silicon was $4.2 \cdot 10^{-6}$ ºC^{-1} which is fairly close to reported values, $3.9 \cdot 10^{-6}$ ºC^{-1} and $4.15 \cdot 10^{-6}$ ºC^{-1}.[33,34]

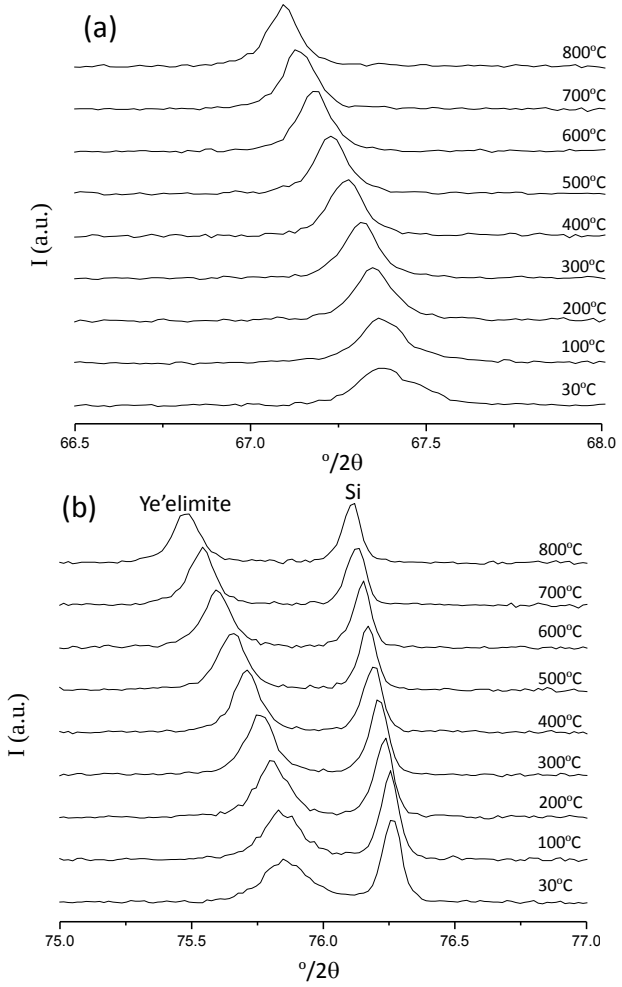

Figure 2. Selected high-angle regions of the VT-LXRPD data for doped ye'elimite. (a) Pseudo-cubic (622) reflection of doped ye'elimite; (b) a second region showing reflections from ye'elimite and Si (internal standard, for details see the text).

Table 3. Linear thermal expansion coefficients for doped and stoichiometric (St.) ye'elimite at different temperatures.

T /ºC	20-450	20-450	20-450	20-400	500-800
α/ºC^{-1}	α_a	α_b	α_c	α_L	α_L
St.	$1.7 \cdot 10^{-6}$	$2.0 \cdot 10^{-6}$	$11.5 \cdot 10^{-6}$	$5.1 \cdot 10^{-6}$	$8.3 \cdot 10^{-6}$
Doped	-	-	-	$6.6 \cdot 10^{-6}$	$9.0 \cdot 10^{-6}$

The 800ºC powder pattern for doped ye'elimite was also auto-indexed using DICVOL06[29] in a cubic unit cell. The results are given in Table 1. Figures of merit[30] for this indexation are much higher than those obtained at RT which points toward a truly cubic structure at high temperature. A Rietveld refinement was performed using the previously reported split-atom model for the sulfate anion[9]. The refinement in space group $I\bar{4}3m$ is very good as indicated by the low R-factors (see Table 2) and the flatness of the difference curve of the Rietveld plot (see Figure 5). However, this structure is not reported as it is essentially identical to that already reported for stoichiometric ye'elimite[9]. The final refined unit cell parameter at 800ºC was a=9.2544(1) Å.

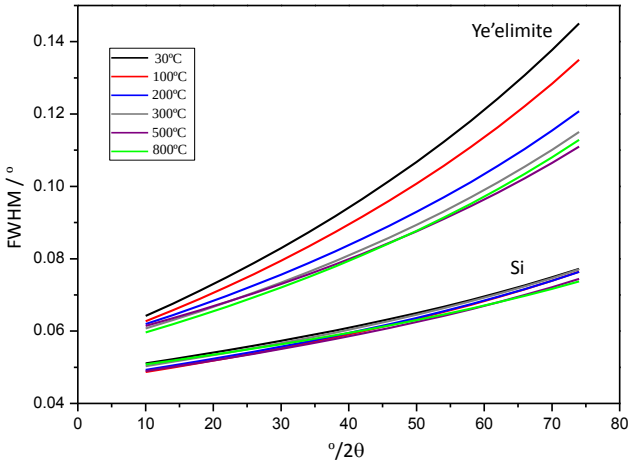

Figure 3. Full-width at the half-maximum variation with temperature for doped ye'elimite and silicon.

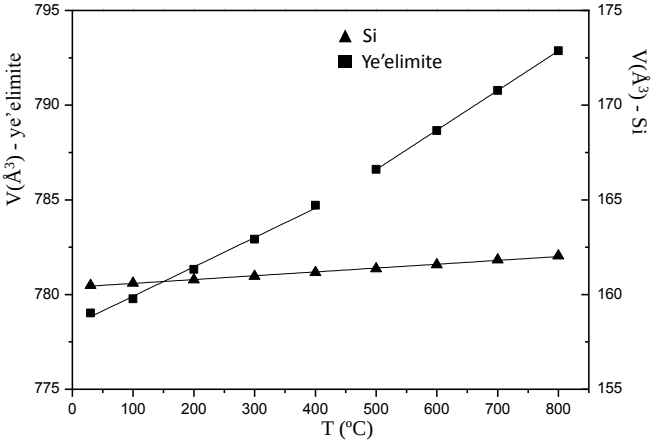

Figure 4. Refined volume for the doped ye'elemite and silicon (internal standard) from RT to 800ºC as a function of temperature. Errors are smaller than the points.

The high-temperature form of stoichiometric ye'elimite has also been thoroughly studied for the sake of comparison. Firstly, the pattern was auto-indexed using DICVOLD06[29] in a cubic unit cell, Table 1. We have not included the peak at 25.5º peak because we have recently noticed that it arises from the sample holder. The absence of this peak in the ye'elimite pattern has been already pointed out[9]. It is worth noticing that the indexing figure of merit[30] values for stoichiometric ye'elimite are higher than those of doped ye'elimite (both patterns were collected in identical conditions and at the same temperature). The cubic structure was verified by fitting the powder pattern with the structure recently reported[9]. Table 2 shows the agreement factors obtained using published[7,9] and refined data. The final unit cell parameter is a=9.2497(1) Å.

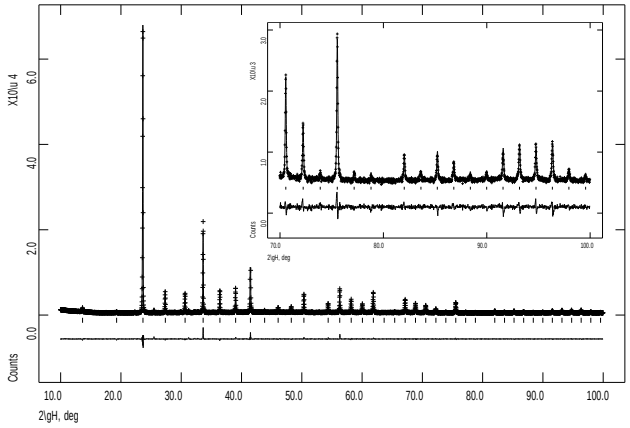

Figure 5. HT-LXRPD plot for doped ye'elimite at 800ºC fitted with a refined cubic crystal structure. Inset detail the high-angle range.

The high temperature crystal structure of doped ye'elimite is cubic. Therefore, if the room temperature structure of this sample is also cubic, no phase transition would be expected of heating. The variable-temperature permittivity study for doped ye'elimite, see Figure 6, shows the presence of a peak at 525ºC, which is an experimental evidence of a phase transition. For the sake of comparison, the similar measurement for stoichiometric ye'elimite is also shown in Figure 6 where the transition is observed at 470ºC.[4] This transition, also observed by differential scanning calorimetry and thermodiffraction was due to the orthorhombic-to-cubic transition and justified by the dynamical disorder of the sulfate anions within the cages.

We justify the change observed at 525ºC for doped ye'elimite as the pseudo-cubic-to-cubic phase transition also related to dynamical disorder of the sulfate anions. The difference in temperature is likely due to the effect of the dopants stabilizing the static disorder of the sulfate anions within the cages.

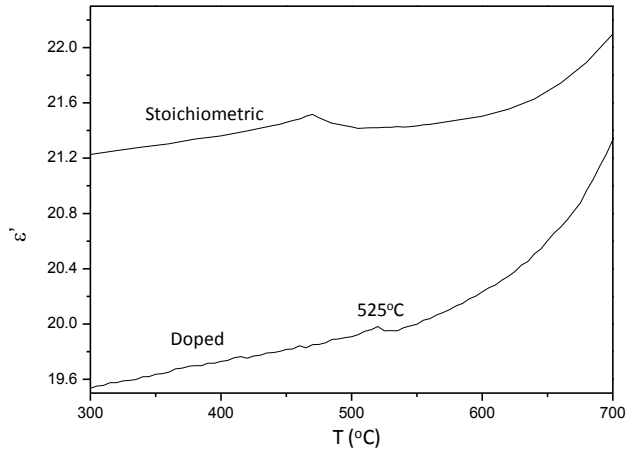

Figure 6. Permittivity signal for stoichiometric ye'elemite and doped ye'elimite.

The complete picture that emerges from this study is that the average high-temperature structure of ye'elimite (both doped and stoichiometric) is cubic. On cooling, stoichiometric ye'elimite undergoes a cubic-to-orthorhombic phase transition at 470ºC likely due to the freezing and spatial ordering of the sulfate anions. The associate splitting of the diffraction peaks is clearly seen in Figure 7. On cooling, doped ye'elimite undergoes a related cubic-to-pseudo cubic phase transition at 525ºC also likely due to the freezing of the sulfate anions. However, the long-range ordering of the sulfate anions does take place, due to the presence of the dopants, and the orthorhombic structure does not develop. Short-range correlations still develop at room temperature and this is evident in the background of the synchrotron pattern (see Figure 7 intermediate panel) as small humps.

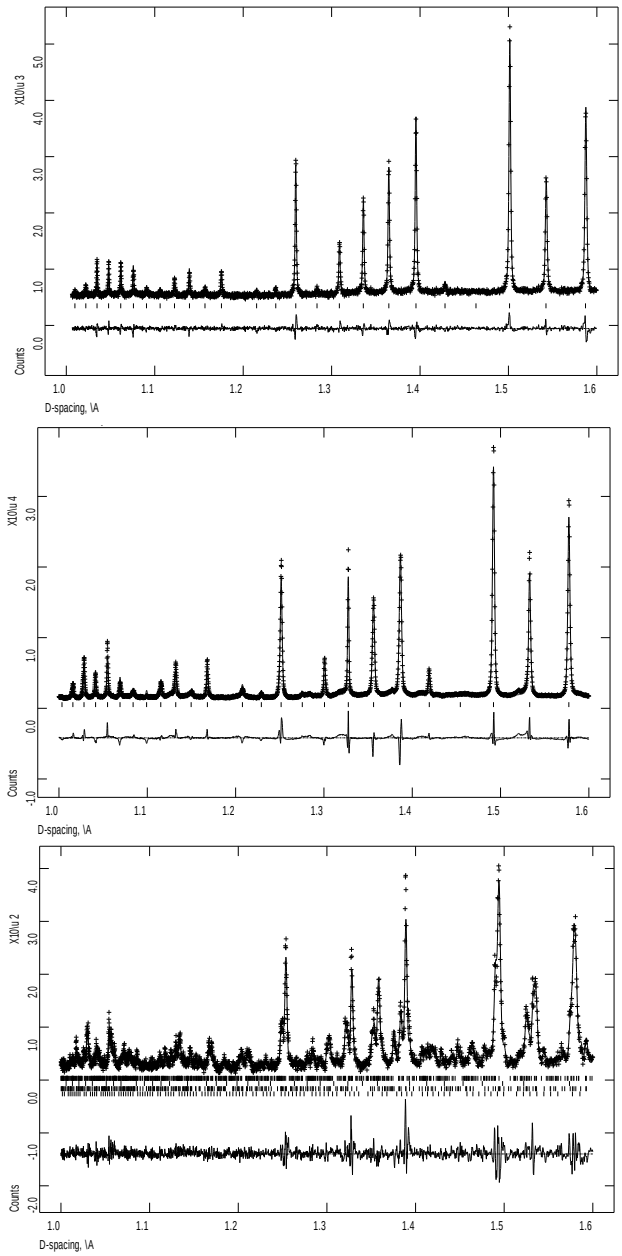

Figure 7. Selected region (1.0 to 1.6 Å) for the LXRPD pattern of doped ye'elimite at 800ºC (top), SXRPD pattern of doped ye'elimite at RT (intermediate), and LXRPD pattern of stoichiometric ye'elimite at RT (bottom).

CONCLUSIONS

The crystal structure of doped ye'elemite, $Ca_{3.8}Na_{0.2}Al_{5.6}Fe_{0.2}Si_{0.2}O_{12}SO_4$, has been studied by high-

resolution synchrotron powder diffraction data. A cubic structural description is reported based on $I\bar{4}3m$ space group with a split-atom model for the sulfate anions. A thermodiffractometric study shows a narrowing of the diffraction peaks on heating with some split peaks at room temperature evolving to single reflections at high temperatures. A variable temperature permittivity study shows a phase transition on heating at 525ºC. The structural study at 800ºC suggests a truly cubic structure and we speculate that the observed phase transition is likely related with the freezing of the sulfate anions on cooling. For stoichiometric ye'elimite, this freezing is accompanied by an ordering of the sulfate anions which provokes the cubic-to-orthorhombic phase transition. However, for doped ye'elimite the freezing is not accompanied by long-range ordering of the sulfate anions but they are locally disordered due to the presence of dopants.

ASSOCIATED CONTENT

Supporting Information. CIF file for the pseudo-cubic crystal structure at room for doped ye'elimite, $Ca_{3.8}Na_{0.2}Al_{5.6}Fe_{0.2}Si_{0.2}O_{12}SO_4$. Table S1 gives the final (refined) atomic parameters (coordinates and anisotropic displacement parameters) and Table S2 the interatomic distances and angles for doped ye'elimite at room temperature. Figure S1 displays the full thermodiffractometric study for doped ye'elimite with Si added as internal standard. Figures S2-S6 display the Rietveld plots for doped ye'elimite at selected temperatures: 30, 100, 300, 500, 700 ºC, respectively.

AUTHOR INFORMATION

Corresponding Author

*g_aranda@uma.es

Author Contributions

This is part of the Ph.D. of Ms. Ana Cuesta. The manuscript was written through contributions of all authors. All authors have given approval to the final version of the manuscript.

Funding Sources

This work has been supported by Spanish Ministry of Science and Innovation through MAT2010-16213 research grant which is cofounded by FEDER and by Junta de Andalucía (Spain) through the P11-FQM-7517 research grant. I. Santacruz thanks a Ramón y Cajal fellowship, RYC-2008-03523. We also thank CELLS-ALBA (Barcelona, Spain) for providing synchrotron beam time at BL04-MSPD and Dr. Fauth for his assistance during the experiment.

REFERENCES

(1) Hurlbut, C. S.; Klein, C. *Manual of Mineralogy*, 20th ed., 1985.
(2) Depmeier,W. *Phys Chem Minerals*. **1988**, *15*, 419–426.
(3) Depmeier,W. *Acta Cryst. B44*, **1988**, 201–207.
(4) Cuesta, A.; De la Torre, A.G.; Losilla, E.R.; Peterson, V.K.; Rejmak, P. ; Ayuela, A.; Frontera, C.; Aranda, M.A.G. *Chem. Mater.* **2013**, *25*, 1680–1687.
(5) Halstead, P.; Moore, A.E. *J. Appl. Chem*. **1962**, *12*, 413–419.
(6) Wang, Y. G.; YE, H.Q.; Kuo, K.H.; Feng, X.J.; Lao, G.L.; Long, S.Z. *J. Mater. Sci*. **1990**, *25*, 5147–5156.
(7) Saalfeld, H.; Depmeier, W. *Kristall and Techinik*, **1972**, *7*, 229–233.
(8) Calos, N.J.; Kennard, C.H.L.; Whittaker, A.K.; Davis, R.L. *J. Solid State Chem.* **1995,** *119*, 1–7.
(9) Kurokawa, D.; Takeda, S.; Colas, M.; Asaka, T.; Thomas, P.; Fukuda, K. *J. Solid State Chem*. **2014**, *215*, 265–270
(10) Hargis, C.W.; Moon, J.; Lothenbach, B.; Winnefeld, F.; Wenk, H-R.; Monteiro, J.M. *J. Am. Ceram. Soc*. **2014**, *97*, 892–898.
(11) Idrissi, M.; Diouri, A.; Damidot, D.; Greneche, J.M.; Alami Talbi, M. ; Taibi, M. *Cem. Concr. Res*. **2010**, *40*, 1314–1319.
(12) Chen, D. ; Feng, X. ; Long. S.; *Thermoc. Acta*, **1993**, *215*, 157–169.
(13) Andac O.; Glasser, F.P. *Adv. Cem. Res*. **1994**, *6*, 57–60.
(14) García-Maté, M. ; Santacruz, I.; De la Torre, A.G.; León-Reina, L.; Aranda, M.A.G. *Cem. Concr. Comp.* **2012**, *34*, 684–691.
(15) García-Maté, M.; De la Torre, A. G.; León-Reina, L.; Aranda, M.A.G.; Santacruz, I. *Cem. Concr. Res.* **2013**, *54*, 12–20.
(16) Odler, I. Special Inorganic Cements, Taylor and Francis, London, 2000.
(17) Álvarez-Pinazo, G.; Santacruz, I.; León-Reina, L.; Aranda, M.A.G.; De la Torre, A.G. *Ind. Eng. Chem. Res*. **2013**, *52*, 16606–16614.
(18) Morin, V.; Walenta, G.; Gartner, E.; Termkhajornkit, P.; Baco, I.; Casabonne, J.M.; Proceedings of the 13th international Congress on the Chemistry of Cement, Madrid, Spain, **2011**.
(19) Cuberos, A.J.M.; De la Torre, A.G.; Álvarez-Pinazo, G.; Martín-Sedeño, M.C.; Schollbach, K.; Pöllmann, H.; Aranda, M.A.G. *Environ. Sci. Technol*. **2010**, 44, 6855–6862.
(20) Gartner, E. *Cem. Concr. Res.* **2004**, *34*, 1489–1498.
(21) Aranda, M.A.G.; De la Torre, A.G.; in *Eco-efficient concrete*; Pacheco-Torgal, F. Ed.; Jalali, S. Ed. Labrincha, J. Ed.; Woodhead Publishing: Cambridge, 2013; 488.
(22) Álvarez-Pinazo, G.; Cuesta, A.; García-Maté, M.; Santacruz, I.; Losilla, E.R.; De la Torre, A.G.; León-Reina, L.; Aranda, M.A.G. *Cem. Concr. Res*. **2012**, *42*, 960–971.
(23) Bullerjahn, F.; Schmitt, D.; Ben Haha, M. *Cem. Concr. Res*. **2014**, *59*, 87–95.
(24) Andac, O.; Glasser, F.P. *Mater. Res. Soc. Symp. Proc*. **1995**, *370*, 135–142.
(25) Touzo, B.; Scrivener, K.L.; Glasser, F.P. *Cem. Concr. Res.* **2013**, *54*, 77–86.
(26) Fauth, F.; Peral, I.; Popescu, C.; Knapp, M. *Powder Diffr*. **2013**, *28*, S360–S370.
(27) Larson, A.C.; Von Dreele, R.B. General Structure Analysis System (GSAS), Los Alamos National Laboratory Report LAUR (2000) pp 86–748.
(28) Thompson, P.; Cox, D.E.; Hasting, J.B. *J. Appl. Cryst.* **1987**, *20*, 79–83.
(29) Boultif, A.; Louer, D. *J. Appl. Crystallogr*. **2004**, *37*, 724–731.
(30) De Wolff, P.M. *J. Appl. Crystallogr*. **1972**, *5*, 243.
(31) Henderson, C.M.B.; Taylor, D. *Phys. Chem. Minerals* **1978**, *2*, 337–347
(32) Marinkovic, B.A.; Jardim, P.M.; Saavedra, A.; Lau, L.Y.; Baehtz, C.; De Avillez, R.R.; Rizzo, F. *Microporous Mesoporous Mater*. **2004**, *71*, 117–124.
(33) Xing, X.; Chen, J.; Deng, J.; Liu, G. *Rare Metals* **2004**, *23*, 364–367.
(34) Straumanis, M.E.: Aka, E.Z. *J. Appl. Phys.* **1952**, *23*, 330–334.

TOC.

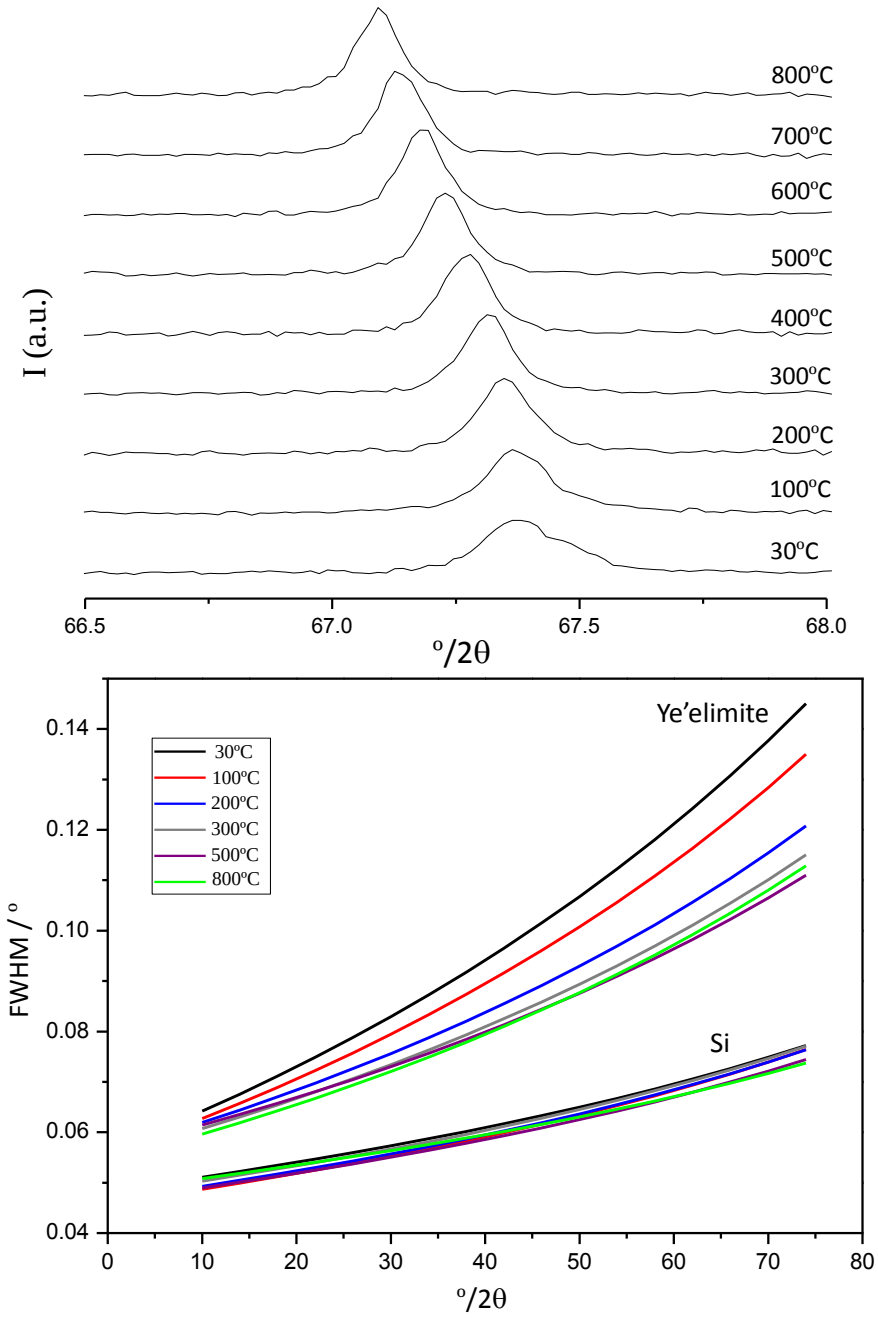

SYNOPSIS TOC TEXT (60 words)**:**

A room-temperature pseudo-cubic structure for doped ye'elimite is reported. The powder pattern of this compound shows narrowing of the diffraction peaks on heating, see figure, which is fully consistent with a measured phase transition at 525ºC. This transition is present in all sodalite compounds.